

A fiber-based, high-power supercontinuum light source

A. K. Abeeluck and C. Headley

OFS Laboratories, 25 Schoolhouse Road, Somerset, New Jersey 08873
abeeluck@ofsoptics.com

C. G. Jørgensen

OFS Fitel Denmark I/S, Priorparken 680, 2605 Brøndby, Denmark

Abstract: High-power supercontinuum generation, based on a highly nonlinear fiber pumped by a continuous-wave Raman fiber laser, is reported. Output powers as high as 3.2 W and bandwidths greater than 544 nm are experimentally demonstrated.

©2003 Optical Society of America

OCIS codes: (060.4370) Nonlinear optics, fibers; (190.4410) Nonlinear optics, parametric processes

1. Introduction

Supercontinuum (SC) generation in optical fibers has been the subject of intensive research over the past few years. Such ultra-broadband light sources are potentially useful for a variety of telecom and non-telecom applications [see Refs. in 1]. Continua with bandwidths greater than 1000 nm have been demonstrated in small effective area optical fibers [2] pumped by pulsed lasers with peak powers of the order of kW. An alternative approach uses continuous-wave (CW) lasers with power levels of the order of a few Watts as the pump sources [1,3,4]. Recently, we demonstrated SC generation over a bandwidth greater than 247 nm in 4.5 km of a highly nonlinear, dispersion-shifted fiber (HNLF) under CW pumping [1]. However, the SC power was limited to about 260 mW at ~ 1 W pump power due to the accumulated material loss in the long fiber.

In this paper, we demonstrate high-power SC generation in shorter lengths of HNLFs pumped by a CW Raman fiber laser (RFL). By varying the HNLF length, the SC power and the bandwidth can be optimized. With a launch power approaching 4 W, a total SC power as high as 3.2 W is achieved with 0.5 km of HNLF while 1.5 km of fiber allows a bandwidth greater than 544 nm. The HNLFs also had shorter zero dispersion wavelengths (λ_0) so that the pump could be placed at a shorter wavelength in the anomalous dispersion regime to generate a spectrum covering the S, C and L bands. The experimental data show that modulation instability (MI) plays an important role in seeding the spectral broadening process at low launch powers while SC generation at high launch powers relies on the interplay between MI and stimulated Raman scattering (SRS).

2. Experimental setup

Figure 1 shows the experimental setup for the generation of the high-power SC. A 915 nm laser diode (LD) bar was used to pump a Yb-doped cladding-pumped fiber laser (CPFL). The 1117 nm light from the CPFL then pumped a cascaded Raman resonator (CRR) that had a nonlinear fiber sandwiched between nested pairs of fiber Bragg gratings (FBGs) to generate five Stokes orders with the final one at 1486 nm being the output of the RFL. Back reflections into the laser cavity were prevented by an optical isolator. A filter was used to suppress the Stokes order at 1590 nm, generated in the CRR at high pump powers from the CPFL. This was necessary as the unfiltered light from the CRR caused further growth of the seed Stokes line in the HNLF through SRS at the expense of the rest of the continuum. The optical filter also eliminated the residual lower order Stokes lines from the CRR output.

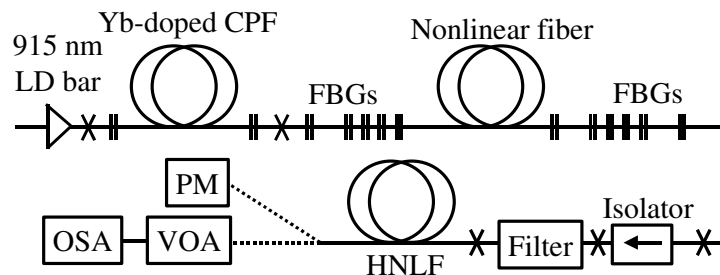


Fig. 1. Experimental setup for SC generation in a HNLF pumped by a high-power CW RFL.

Continuum generation was studied in three HNLFs of lengths $L = 0.5$ km, 1 km and 1.5 km as a function of the launch power from the RFL, P_{RFL} , that takes into account the splice loss between the filter and the HNLF. Each

HNLF had a Ge-doped silica core with a depressed F-doped inner cladding. The effective modal area is typically $\sim 10\text{-}12 \mu\text{m}^2$ at 1550 nm, thus allowing an enhancement of nonlinear effects. The average λ_0 and the dispersion slope (S_0) of each fiber are listed in Table 1. The SC light was attenuated using a free-space variable optical attenuator (VOA), and the spectral evolution of the continuum was recorded on an optical spectrum analyzer (OSA), set at its highest resolution bandwidth of 0.05 nm. The experimental transfer function (total SC power versus launch power) of each HNLF was determined using a calorimetric power meter (PM) that had a wavelength range of 0.19-10.6 μm .

Table 1. Comparison of the properties of continua generated in three different lengths of HNLFs.

L (km)	λ_0 (nm)	S_0 (ps/nm ² /km)	$\beta_{2,\text{expt.}}(\omega_p)$ (ps ² /km)	$\beta_{2,\text{fit.}}(\omega_p)$ (ps ² /km)	Launch power (W)	Bandwidth (nm)	Spectral flatness (dB)	SC power (W)	ξ
0.5	1481	0.029	-0.17	-0.16	3.97	> 312	< 6.0	3.20	81%
1.0	1481	0.026	-0.15	-0.16	3.86	> 505	< 2.4	2.54	66%
1.5	1478	0.027	-0.25	-0.18	3.87	> 544	< 3.8	1.89	49%

3. Results and discussion

Figure 2 displays the growth of the SC for each length of HNLF at similar launch powers that are indicated next to each spectrum. The power along the vertical axis has been normalized to the maximum spectral power across each recorded spectrum. The laser spectrum broadens beyond the limit of the OSA at 1770 nm with increasing P_{RFL} .

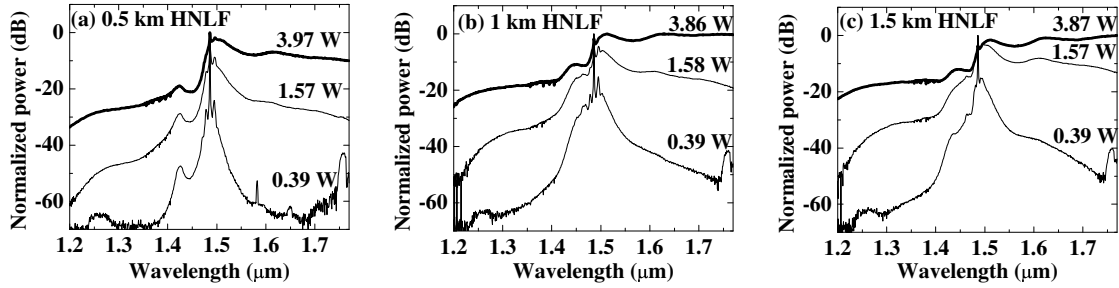


Fig. 2. Continuum growth as a function of launch power (shown against each spectrum) in a HNLF of length (a) 0.5 km, (b) 1 km, and (c) 1.5 km.

The pump wavelength is positioned in the anomalous dispersion regime of each HNLF so that MI, interpreted as four-wave mixing phase-matched by self-phase modulation, can occur. Indeed, the characteristic sidelobes [5] due to MI are clearly visible in Fig. 2. To first order in the Taylor expansion of the material dispersion contribution, the net wavevector mismatch κ can be expressed as $\kappa = \beta_2 \Omega_s^2 + 2\gamma P_{\text{RFL}} = 0$, where β_2 is the group velocity dispersion coefficient at the pump laser frequency (ω_p), Ω_s is the frequency shift that provides the locations of the MI sidelobes ($\omega_{\pm} = \omega_p \pm \Omega_s$), and γ is the effective nonlinearity [5]. The wavelengths at which maximum parametric gain occurs were calculated for each HNLF at $P_{\text{RFL}} = 0.39 \text{ W}$ using the phase-matching condition with β_2 as a fitting parameter and assuming $\gamma = 10.6 \text{ W}^{-1}\text{km}^{-1}$. The fitted values of β_2 agree well with those determined from the experimentally measured fiber dispersions (see table 1). In the low launch power regime, MI is the dominant mechanism for spectral broadening. With a longer interaction length, the laser light also undergoes SRS, as observed by the growth of a low-intensity peak in the vicinity of 1590 nm in Fig. 2 (c) for $P_{\text{RFL}} = 0.39 \text{ W}$.

Phase matching at larger values of P_{RFL} requires Ω_s to increase. Thus, the longer wavelength MI peak starts overlapping the Raman gain spectrum of the pump laser and is amplified through SRS [5]. This explains the asymmetric growth of the MI sidelobes at higher launch powers with the progressive depletion of the pump laser. With $P_{\text{RFL}} = 3.87 \text{ W}$, the phase-matching condition and the material parameters predict that the amplified MI sidelobe should occur at $\sim 1513 \text{ nm}$, as confirmed experimentally. The growth of a peak around 1624 nm indicates that, in the high launch power regime, the amplified MI sidelobe acts as a pump for the generation of a Stokes order through SRS. A second Stokes order around 1750 to 1770 nm is also observed with the 1 km and 1.5 km HNLFs. Further enhancement of these Stokes orders through SRS in the longer 1.5 km HNLF at $P_{\text{RFL}} = 3.87 \text{ W}$ leads to the depletion of the Raman-amplified MI peak. Under a high-power CW pumping condition, the continuum grows in the normal dispersion regime as well, but to a lesser extent compared to the anomalous dispersion regime where the continuum generation process takes advantage of the combined effects of MI and SRS.

The 20-dB bandwidth and the spectral flatness in the wavelength range from 1520 nm to 1770 nm are shown in table 1 for each HNLF at the highest value of P_{RFL} . The bandwidth increases with increasing fiber length since the components of the initially broadened spectrum can interact further in the longer HNLF to produce more broadening. A bandwidth greater than 544 nm was thus obtained with $L = 1.5$ km at $P_{RFL} = 3.87$ W. Table 1 and Fig. 2 indicate that the spectral flatness can be controlled over a given wavelength range by optimizing the fiber length and the launch power. With 1 km of HNLF and $P_{RFL} = 3.86$ W, the spectrum from 1520 nm to 1770 nm was flat to within < 2.4 dB. Further spectral shaping can be performed using concatenated long period gratings.

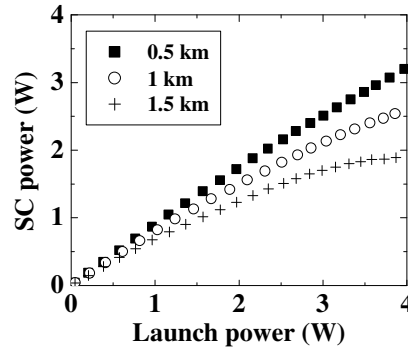


Fig. 3. Experimental transfer functions of the SC light source for HNLF lengths of 0.5 km, 1 km and 1.5 km.

The transfer function of the SC source was experimentally determined as a function of the HNLF length, and the results are shown in Fig. 3. The SC power increases linearly for small values of P_{RFL} . The transfer function becomes nonlinear for higher launch power levels. The deviation from linearity occurs at a lower value of P_{RFL} for the longer HNLF. This is due to the fact that with a longer fiber the initial laser power is distributed more and more over longer wavelengths (> 1700 nm) that experience larger material losses, thereby reducing the total output power. Table 1 shows how the SC power and the conversion efficiency ($\xi = \text{SC power/launch power}$) vary as a function of fiber length. A SC power of 3.2 W and a conversion efficiency of 81% are achieved with $L = 0.5$ km. The table also clearly demonstrates the tradeoff between the bandwidth and the total SC power under the given experimental conditions. These properties can be optimized by varying the fiber length and the launch power. Broadband light sources with large output powers are highly desirable for applications such as the interrogation of FBG sensors distributed over several kilometers. The large bandwidth allows the multiplexing of a higher density of sensing elements while the high power allows for a larger signal-to-noise ratio of the reflected light.

4. Summary

High-power SC generation is experimentally demonstrated in short lengths of HNLFs pumped by a CW RFL. It is shown that at a given pump power, the SC power and the bandwidth can be maximized individually by varying the fiber length. Thus, a SC power of 3.2 W and a bandwidth greater than 544 nm are experimentally demonstrated in 0.5 km and 1.5 km of HNLFs, respectively. The experimental data also show that spectral broadening occurs mainly through MI at low launch powers while the interplay between SRS and MI leads to the continuum growth in the high launch power regime.

References

1. A. K. Abeeluck, S. Radic, K. Brar, J.-C. Bouteiller, and C. Headley, "Supercontinuum Generation in a Highly Nonlinear Fiber Using a Continuous Wave Pump," in *OSA Trends in Optics and Photonics (TOPS) Vol. 86, Optical Fiber Communication Conference*, Technical Digest, Postconference Edition (Optical Society of America, Washington, DC, 2003), pp. 561-562.
2. J. K. Ranka, R. S. Windeler, and A. J. Stentz, "Visible continuum generation in air-silica microstructure optical fibers with anomalous dispersion at 800 nm," *Opt. Lett.* **25**, 25-27 (2000).
3. M. Prabhu, N. S. Kim, and K. Ueda, "Ultra-Broadband CW Supercontinuum Generation centered at 1483.4 nm from Brillouin/Raman Fiber Laser," *Jpn. J. Appl. Phys.* **39**, L291-L293 (2000).
4. T. J. Ellingham, L. M. Gleeson, and N. J. Doran, "Enhanced Raman amplifier performance using nonlinear pump broadening," *ECOC 2002*, **2**, Paper 4.1.3 (2002).
5. G. P. Agrawal, *Nonlinear Fiber Optics* (Academic Press, 1995).